

# Perfusion MRI in Treatment Evaluation of Glioblastomas: Clinical Relevance of Current and Future Techniques

Bart R.J. van Dijken, BSc,<sup>1</sup> Peter Jan van Laar, MD, PhD,<sup>1</sup> Marion Smits, MD, PhD,<sup>2</sup>  
Jan Willem Dankbaar, MD, PhD,<sup>3</sup> Roelien H. Enting, MD, PhD,<sup>4</sup> and  
Anouk van der Hoorn, MD, PhD<sup>1,5\*</sup>

CME

## CME Information: Perfusion MRI in treatment evaluation of glioblastomas, clinical relevance of current and future techniques

If you wish to receive credit for this activity, please refer to the website: [www.wileyhealthlearning.com](http://www.wileyhealthlearning.com)

### Educational Objectives

Upon completion of this educational activity, participants will be better able to interpret perfusion MRI images for treatment evaluation of glioblastomas and describe the advantages and pitfalls of the most commonly employed perfusion MRI techniques.

### Activity Disclosures

No commercial support has been accepted related to the development or publication of this activity.

### Faculty Disclosures:

**Editor-in-Chief:** Mark E. Schweitzer, MD, discloses consultant fees from MCRA and MMI.

**CME Editor:** Mustafa R. Bashir, MD, discloses research support from GE Healthcare, Madrigal Pharmaceuticals, NGM Biopharmaceuticals, Siemens Healthcare and Taiwan J Pharma, and consultant fees from RadMD.

### CME Committee:

Bonnie Joe, MD, PhD, discloses author royalties from UpToDate.

Tim Leiner, MD, PhD, discloses research grants from Bayer Healthcare and Philips Healthcare.

Shreyas Vasanawala, MD, PhD, discloses research support from GE Healthcare, and founder's equity in Arterys.

Eric Chang, MD, Feng Feng, MD, and Bruno Madore, PhD; no conflicts of interest or financial relationships relevant to this article were reported.

### Authors:

BRJ van Dijken, PJ van Laar, M Smits, JW Dankbaar, RH Enting, and A van der Hoorn reported no conflicts of interest or financial relationships relevant to this article.

This activity underwent peer review in line with the standards of editorial integrity and publication ethics. Conflicts of interest have been identified and resolved in accordance with John Wiley and Sons, Inc.'s Policy on Activity Disclosure and Conflict of Interest.

### Accreditation

John Wiley and Sons, Inc. is accredited by the Accreditation Council for Continuing Medical Education to provide continuing medical education for physicians.

John Wiley and Sons, Inc. designates this journal-based CME activity for a maximum of 1.0 *AMA PRA Category 1 Credit*<sup>™</sup>. Physicians should only claim credit commensurate with the extent of their participation in the activity.

For information on applicability and acceptance of continuing medical education credit for this activity, please consult your professional licensing board.

This activity is designed to be completed within 1 hour. To successfully earn credit, participants must complete the activity during the valid credit period, which is up to two years from initial publication. Additionally, up to 3 attempts and a score of 70% or better is needed to pass the post test.

View this article online at [wileyonlinelibrary.com](http://wileyonlinelibrary.com). DOI: 10.1002/jmri.26306

Received Jun 6, 2018, Accepted for publication Jul 30, 2018.

\*Address reprint requests to: A.v.d.H., Department of Radiology (EB44), University Medical Center Groningen, Hanzeplein 1, P.O. Box 30.001, 9700 RB Groningen, the Netherlands. E-mail: [a.van.der.hoorn@umcg.nl](mailto:a.van.der.hoorn@umcg.nl)

Contract grant sponsor: University of Groningen with a Mandema grant (to A.H.) and Junior Scientific Masterclass grant (to B.D.).

From the <sup>1</sup>Department of Radiology, Medical Imaging Center (MIC), University Medical Center Groningen, Groningen, the Netherlands; <sup>2</sup>Department of Radiology and Nuclear Medicine, Erasmus Medical Center, Rotterdam, the Netherlands; <sup>3</sup>Department of Radiology, University Medical Center Utrecht, Utrecht, the Netherlands; <sup>4</sup>Department of Neurology, University Medical Center Groningen, Groningen, the Netherlands; and <sup>5</sup>Brain Tumour Imaging Group, Division of Neurosurgery, Department of Clinical Neurosciences, University of Cambridge and Addenbrooke's Hospital, Cambridge, UK

This is an open access article under the terms of the Creative Commons Attribution-NonCommercial License, which permits use, distribution and reproduction in any medium, provided the original work is properly cited and is not used for commercial purposes.

Treatment evaluation of patients with glioblastomas is important to aid in clinical decisions. Conventional MRI with contrast is currently the standard method, but unable to differentiate tumor progression from treatment-related effects. Pseudoprogression appears as new enhancement, and thus mimics tumor progression on conventional MRI. Contrarily, a decrease in enhancement or edema on conventional MRI during antiangiogenic treatment can be due to pseudoresponse and is not necessarily reflective of a favorable outcome. Neovascularization is a hallmark of tumor progression but not for posttherapeutic effects. Perfusion-weighted MRI provides a plethora of additional parameters that can help to identify this neovascularization. This review shows that perfusion MRI aids to identify tumor progression, pseudoprogression, and pseudoresponse. The review provides an overview of the most applicable perfusion MRI methods and their limitations. Finally, future developments and remaining challenges of perfusion MRI in treatment evaluation in neuro-oncology are discussed.

**Level of Evidence:** 3

**Technical Efficacy:** Stage 4

J. MAGN. RESON. IMAGING 2019;49:11–22.

**G**LIOMASTOMAS (GBMs) are highly malignant brain tumors with a poor prognosis.<sup>1</sup> It is important to distinguish patients with a GBM who respond to treatment from patients who do not respond to treatment. Patients who do not respond to treatment can undergo an expensive and potentially harmful treatment, which should thus be discontinued. Moreover, clinical trials investigating new therapeutic agents should rely on adequate evaluation of treatment response. It is currently not possible to reliably differentiate tumor progression from treatment-related changes with conventional imaging techniques. Improvement of treatment evaluation in neuro-oncology is therefore necessary.

Treatment response evaluation in neuro-oncology is highly dependent on imaging. Magnetic resonance imaging (MRI) with its excellent soft-tissue contrast, high spatial resolution, and widespread availability has become the standard method. However, conventional MRI has one important limitation: the inability to differentiate tumor from treatment-related changes.<sup>2</sup> Tumor progression will most often result in increased enhancement on postcontrast MRI. However, enhancement can also be due to a treatment-related blood-brain barrier disruption without underlying tumor progression. This is called pseudoprogression.<sup>3,4</sup> Furthermore, antiangiogenic treatment can result in a decrease of enhancement on postcontrast MRI while the tumor remains stable or even

increases. This is called pseudoresponse. Thus, posttherapeutic effects such as pseudoprogression and pseudoresponse hinder a reliable treatment evaluation.

Perfusion-weighted MRI provides a plethora of additional parameters to overcome the shortcomings of conventional MRI. Perfusion MRI can be used to image neovascularization, a hallmark of tumor progression. The net result of neovascularization is an extensive network of poorly organized tumor vessels. Tumor vessels are tortuous, often large and uneven in diameter, slow flowing, and leaky.<sup>5–7</sup> Leakage of contrast from tumor vessels is visible as enhancement on conventional postcontrast T<sub>1</sub>-weighted MRI. However, with perfusion MRI it is possible to determine the blood volume and flow as well as the leakage component, thereby extending information about the tumor vasculature. This review will show the potential value of perfusion MRI during treatment evaluation of GBMs. The different perfusion techniques with their advantages and disadvantages are discussed. Finally, novel perfusion techniques and future challenges are addressed.

## PERFUSION TECHNIQUES

The most frequently used perfusion MRI techniques include dynamic susceptibility contrast (DSC) imaging (Figs. 1–2),

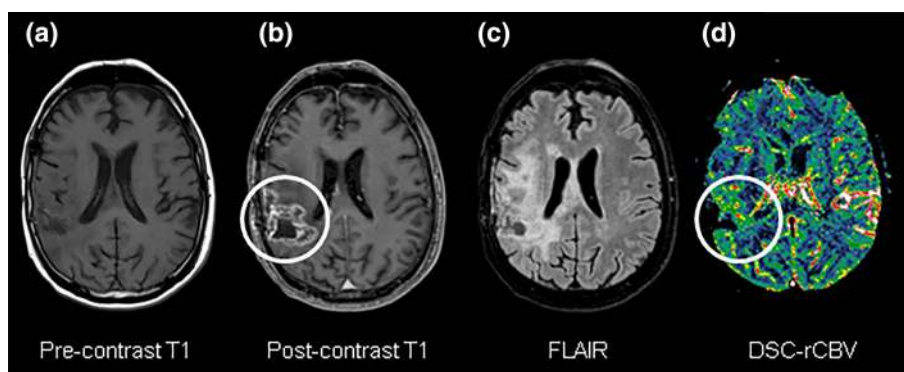


**FIGURE 1:** Dynamic susceptibility contrast (DSC) case of tumor progression. A case of tumor progression in a 68-year-old male after 3 months postchemoradiotherapy. Anatomical MRI pre- (a) and postcontrast (b) T<sub>1</sub>-weighted imaging demonstrated new enhancement and increased FLAIR signal (c) Dynamic susceptibility contrast (DSC) perfusion imaging (d) confirmed tumor progression with elevated rCBV values located at the place of contrast enhancement as indicated by the white circles. DSC = dynamic susceptibility contrast, rCBV = relative cerebral blood volume.

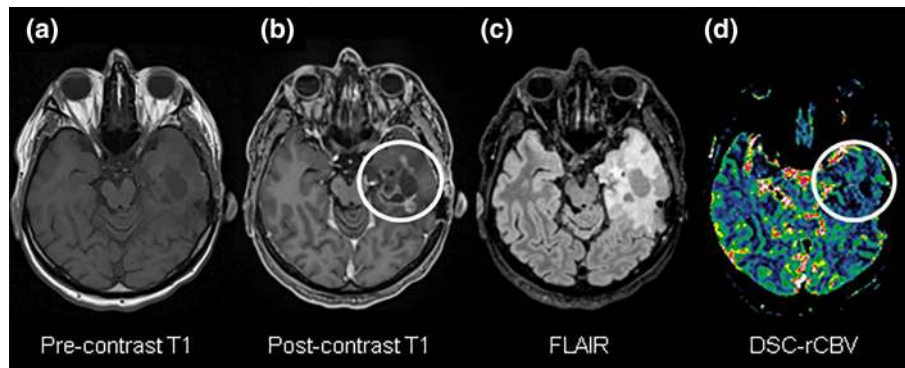


**FIGURE 2:** Dynamic susceptibility contrast (DSC) in a patient with pseudoprogession. Pseudoprogession in a 35-year-old male 6 months after completion of chemoradiotherapy. Pre- (a) and postcontrast T<sub>1</sub>-weighted imaging (b) and FLAIR (c) were both suggestive of apparent progressive disease. However, DSC (d) correctly showed that these changes were due to pseudoprogession, as rCBV values were not elevated at the location of the enhancing lesion (white circles). DSC = dynamic susceptibility contrast, rCBV = relative cerebral blood volume.

dynamic contrast-enhanced (DCE) imaging, and arterial spin labeling (ASL) (Fig. 3). An overview of the different perfusion techniques and their advantages and limitations is shown in Table 1.

### Dynamic Susceptibility Contrast

DSC is the most widely applied perfusion method.<sup>8,9</sup> DSC is acquired with rapid echo planar imaging (EPI) and relies on a drop in T<sub>2</sub><sup>\*</sup> signal after passage of a gadolinium-based contrast bolus.<sup>10</sup> The loss in the signal intensity–time curve due to susceptibility effects of the contrast agent corresponds to the concentration of the contrast agent. DSC can be performed on both 1.5T and 3T systems. A bolus of contrast agent (0.1 mmol/kg) should be administered ~20 seconds (5–30) after the start of acquisition at a minimal injection rate of 3 mL/s.<sup>11,12</sup> The use of a preload bolus is also recommended to limit leakage effects in DSC, with a ¼ dosage given as preload at the same injection rate 5–10 minutes prior to the ¾ remaining bolus.<sup>12</sup> Various hemodynamic parameters can be calculated from the concentration–time curves.<sup>11</sup> The relative cerebral blood volume in a given amount of tissue (rCBV) is the most studied parameter.<sup>13</sup> The ratio of

rCBV compared with contralateral normal-appearing white matter is often calculated for quantification. Other parameters are relative cerebral blood flow (rCBF), the volume of blood in a given amount of tissue per unit of time, and mean transit time (MTT), the average time red blood cells spend within a determinate volume of capillaries, which can be calculated by dividing the rCBV by the rCBF. Less frequently studied DSC-derived parameters include relative peak height, the difference in baseline signal intensity and minimum signal intensity in the perfusion curve, and percentage of signal recovery, which corresponds to the degree of residual T<sub>2</sub><sup>\*</sup> signal loss.

DSC acquisition can be achieved relatively fast and is widely available compared with other perfusion techniques.<sup>8</sup> Absolute quantification, however, can be troublesome and manual region selection is necessary, making the technique user-dependent. DSC relies on the assumption that the contrast agent remains intravascular. Extravasation of the contrast agent due to the disrupted blood–brain barrier in GBM leading to T<sub>1</sub>- and T<sub>2</sub><sup>\*</sup>-relaxation effects can cause an underestimation or overestimation of rCBV, respectively.<sup>14</sup> The use of a preload contrast bolus and leakage correction algorithms

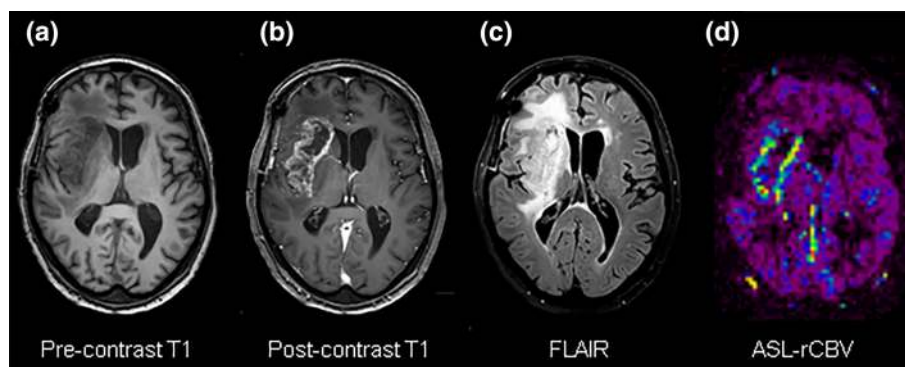


**FIGURE 3:** Arterial spin labeling (ASL) in recurrent glioblastoma. Follow-up imaging of a 40-year-old female with a glioblastoma 3 months after partial resection and chemoradiotherapy. Pre- (a) and postcontrast T<sub>1</sub>-weighted (b) and FLAIR (c) images showed a significant increase of the lesion. ASL perfusion imaging (d) was in accordance with the anatomical images, demonstrating increased CBF values (yellow) corresponding with tumor progression. ASL = arterial spin labeling, rCBF = cerebral blood flow.

**TABLE 1. Overview of Perfusion MRI Methods in Treatment Evaluation of Glioblastoma**

	DSC	DCE	ASL
Sequence	T2* EPI	T1 spoiled-GRE	T1 EPI, FSE
Slice thickness	3–5 mm	2–10 mm	5–10 mm
Temporal resolution	1–1.5 sec	4–6 sec	3–5 sec
Contrast injection rate	3–5 mL/s	2–4 mL/s	No contrast
Acquisition time	2–3 min	3–7 min	4–10 min
Parameters	rCBV rCBF MTT PH PSR	$K^{trans}$ $V_e$ $V_p$ AUC	rCBF ATT
Advantages	short acquisition time widely available visually inspection	microvascular permeability higher spatial resolution	no leakage correction needed no contrast required
Disadvantages	quantification user-dependent susceptibility artifacts	postprocessing complex pharmacokinetic modeling	low signal-to-noise ratio risk of movement artifacts

ASL = arterial spin labeling, ATT = arterial transit time, AUC = area under the curve, DCE = dynamic contrast enhanced, DSC = dynamic susceptibility contrast, EPI = echo planar imaging, FSE = fast spin echo, GRE = gradient echo,  $K^{trans}$  = volume transfer coefficient, MMT = mean transfer time, PH = peak height, PSR = percentage of signal recovery, rCBF = cerebral blood flow, rCBV = relative cerebral blood volume,  $V_e$  = extravascular volume,  $V_p$  = plasma volume.

partially balance these leakage effects.<sup>14,15</sup> Other intravascular contrast agents such as an ultrasmall superparamagnetic iron oxide or an albumin-binding agent have also been studied to tackle the issue of leakage effects.<sup>16,17</sup> Ultrasmall superparamagnetic iron oxide particles are larger than gadolinium

compounds and hence remain intravascular, even when disruption of the blood–brain barrier is present. The downside of these agents, however, is that they do not allow measures of permeability and extracellular volume, and little experience with these agents exist. Furthermore, susceptibility artifacts

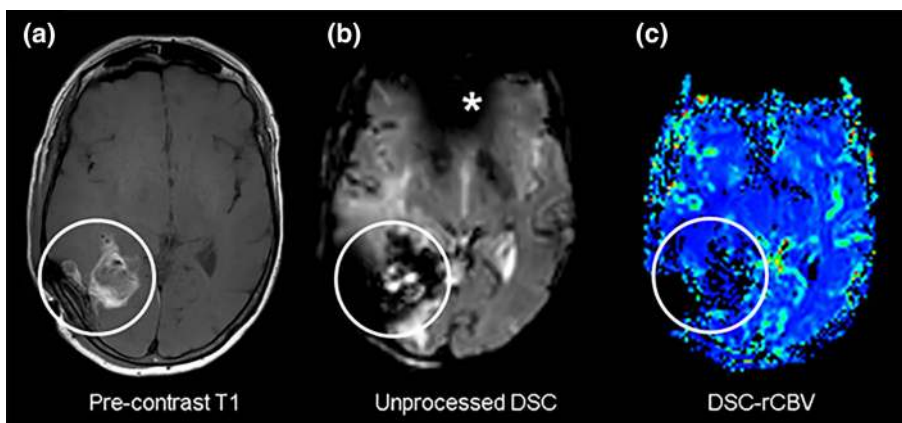


**FIGURE 4:** Susceptibility artifact on dynamic susceptibility contrast (DSC) perfusion MRI. Postoperative imaging after resection of a glioblastoma in a 65-year-old female. The resection cavity contains a hemorrhage (circle) as demonstrated on precontrast T<sub>1</sub>-weighted imaging (a). Unprocessed DSC imaging demonstrated a large susceptibility artifact in the area of the blood products and surgical material after craniotomy (b). The calculated DSC-rCBV is therefore not assessable with artifactual low values (c). Note also a susceptibility artifact frontally (asterisk) due to the skull base and frontal sinuses with bone-air interfaces (b). DSC = dynamic susceptibility contrast, rCBV = relative cerebral blood volume.

occur frequently with DSC. Based on the  $T_2^*$  acquisition of DSC, there is a signal loss due to blood products, calcifications, and aerated structures. As blood is often present within the resection cavity postoperatively, this potentially hinders a reliable interpretation (Fig. 4).

### Dynamic Contrast-Enhanced

With DCE  $T_1$ -weighted spoiled gradient-recalled echo, images are acquired during the administration of a gadolinium-based contrast agent with an injection rate of 2–4 mL/s.<sup>11,18</sup> A signal-intensity curve results from the acquisition and is reflective of perfusion, permeability, and extravascular volume measures. Due to the increased permeability of tumor vasculature, intravascular fluid will leak into the extravascular extracellular space.<sup>18</sup> The parameters that can be calculated from DCE images are the volume transfer coefficient from the blood plasma to the extracellular space ( $K^{\text{trans}}$ ), the extracellular volume ( $V_e$ ), plasma space volume ( $V_p$ ), and area under the curve (AUC).<sup>2,11</sup> Basic features of the signal-intensity curve such as AUC can be extracted easily without the need of a model. However, calculation of most quantitative DCE parameters requires pharmacokinetic modeling. It is possible to incorporate DCE imaging in a multisequence protocol along with DSC. Performing DCE before DSC is recommended, as the first contrast injection then functions as a preload bolus and simultaneously allows calculations of permeability.<sup>11</sup>

DCE is said to better and more completely demonstrate angiogenesis processes, as it is capable of showing microvascular permeability. Furthermore, quantitative assessment of the blood–brain barrier is possible with DCE. As DCE is acquired with a  $T_1$ -weighted sequence, it has a lower temporal resolution than DSC (Table 1). The lower temporal resolution of DCE may not be optimal to adequately extract all parameters.<sup>18</sup> Other disadvantages of DCE include postprocessing and quantification of the images, as there is currently no consensus for the optimal pharmacokinetic model.<sup>19</sup> The Tofts-Kermode model and Extended Tofts-Kermode model are the best-established models, but many more are available.<sup>19,20</sup> It is known that different pharmacokinetic models lead to different measures of  $K^{\text{trans}}$ .<sup>18</sup> Therefore, parameters acquired by different models are not intercomparable. Moreover, pharmacokinetic models require an arterial input function. Determination of the arterial input function is not straightforward and often still relies on manual input.<sup>21</sup> Differences of these variables across institutions hinder reproducibility and generalizability.

### Arterial Spin Labeling

Contrary to the aforementioned techniques, ASL is not dependent on exogenous contrast agents, and thus is completely noninvasive. In ASL, water molecules from arterial blood are magnetically labeled and followed till they arrive in the tissue of interest.<sup>22</sup> The signal difference between the labeled images and separately acquired control images can be

used to compute CBF values.<sup>23</sup> Several methods of ASL imaging currently exist but pseudocontinuous ASL is now widely accepted as the method of choice.<sup>22,24</sup> In pseudocontinuous ASL a relatively long labeling time (2–4 sec) is used consisting of a series of very short radiofrequency pulses, with a spacing of 1 msec between pulses.<sup>24</sup> After a postlabeling delay of 1.5–2 seconds, allowing the labeled blood to arrive in the brain tissue, the images are acquired.<sup>22,25</sup> All arterial blood has equal  $T_1$  decay, as it is continuously inverted as it passes through the labeling plane, making pseudocontinuous ASL superior to other ASL methods.<sup>23</sup> The labeling plane should be placed in a region with relatively straight feeding arteries perpendicular to the labeling plane.<sup>22,24</sup> Traditionally, EPI was used to acquire ASL, but nowadays fast spin echo and 3D gradient and spin echo can be applied with the advantage of single-shot acquisition.<sup>22</sup> Although ASL is also possible on 1.5T MR systems, 3T scanners reach a higher signal to noise ratio (SNR) and are therefore preferred.

A major advantage of ASL compared with other perfusion techniques is the avoidance of leakage effects. Leakage correction, such as in DSC, is not needed in ASL, as the tracer (water) is diffusible.<sup>11,23</sup> Direct beneficial effects of contrast avoidance are limited as GBM patients receive contrast for anatomical MRI acquisition. Even though the SNR is lower in pseudocontinuous ASL than pulsed ASL, SNR in ASL is still lower compared with DSC and DCE. Therefore, the scan time is prolonged in ASL with the consequential risk of movement artifacts.<sup>11</sup> Other frequently occurring artifacts include susceptibility artifacts, blurring, and diminished background suppression.<sup>25</sup> Furthermore, the number of parameters that can be generated with ALS are limited, with CBF being the most frequently generated parameter. However, it has been shown that ASL-derived CBF values correlate well with rCBV values acquired with DCS perfusion.<sup>22</sup> Other parameters such as arterial transit time<sup>26</sup> are also producible with ASL, but their clinical relevance remains to be further explored.

## PSEUDOPROGRESSION

Pseudoprogression is a transient treatment effect appearing as new enhancement on conventional postcontrast MRI, thereby mimicking tumor progression. Pseudoprogression is a frequently encountered problem; a recent meta-analysis reported the incidence of pseudoprogression during standard treatment<sup>1</sup> to be 36% (95% confidence interval [CI] 33–40) in GBM.<sup>27</sup> Even higher rates of pseudoprogression were reported in patients with methylated O6-methylguanine methyltransferase (MGMT) status and wildtype isocitrate dehydrogenase (IDH) gene status.<sup>3,28</sup> Pseudoprogression typically occurs within 3 months after termination of treatment and is usually transient. However, delayed effects up to years after treatment can be seen. This radiation necrosis is often

progressive and irreversible.<sup>3</sup> Pseudoprogression is most likely the result of vasodilatation, a disrupted blood–brain barrier, and vasogenic edema due to radiation and chemotherapy damage.<sup>3</sup> In radiation necrosis, irreversible fibronoid necrosis, fibrosis, reactive gliosis, demyelination, and vascular hyalinization are seen.<sup>29</sup> Although radiotherapy planning has become more and more precise in minimizing exposure of healthy brain tissue, damage to noncancerous brain is inevitable due to the infiltrative nature of GBMs. Clinically, pseudoprogression can be accompanied by a variety of clinical symptoms, such as headache, nausea, emesis, and neurological deficits. This further complicates the distinction from tumor progression, as these symptoms can also accompany tumor progression. The distinction between pseudoprogression and early tumor progression therefore remains a clinical challenge in posttherapeutic neuro-oncology.

Perfusion MRI is more reliable than conventional MRI in the differentiation between pseudoprogression and tumor progression. A recent meta-analysis demonstrated a pooled sensitivity and specificity of 87% (95% CI 82–91) and 86% (77–91) for DSC and 92% (73–98) and 85% (76–92) for DCE, respectively.<sup>30</sup> The limited studies available for ASL to differentiate tumor progression from pseudoprogression showed a sensitivity ranging from 52–79% and a specificity ranging from 64–82%.<sup>30</sup> A table listing key information of included clinical studies/surveys such as authors, study design including MRI techniques and patient population, major findings, and year of publication can be found in our recent meta-analysis.<sup>30</sup>

The most validated DSC parameter is rCBV. Although CBV can be visually inspected,<sup>31</sup> it is usually quantified using contralateral values to normalize values.<sup>10</sup> Several studies have

shown that rCBV values are higher in tumor progression (Fig. 1) than treatment effects (Fig. 2).<sup>30,32,33</sup> rCBV is high in tumor, as it is reflective of the tumor hyperperfusion volume. However, the optimum rCBV threshold for differentiating between tumor and treatment effects varies significantly between studies (range 0.71–3.7).<sup>30</sup> rCBF can also be collected with DSC imaging but is not often applied in neuro-oncology treatment evaluation. Only one study reported the use of DSC-derived rCBF for differentiating tumor recurrence from stable disease with diagnostic accuracy comparable to rCBV.<sup>34</sup> Other DSC-derived parameters such as peak height and percentage of signal recovery were significantly higher in tumor progression than pseudoprogression.<sup>35–37</sup> However, these parameters were all outperformed by rCBV.<sup>2,30</sup>

DCE demonstrates an even higher diagnostic accuracy for differentiating pseudoprogression from tumor progression.<sup>30</sup> This can in part be explained by the parameter  $K^{trans}$ , which is thought to reflect the increased capillary permeability of leaky tumor vessels. Along with  $K^{trans}$ , most experience is gained with AUC for DCE. Bisdas et al prospectively compared  $K^{trans}$  and AUC in 18 treated high-grade glioma patients and found higher sensitivity and specificity of  $K^{trans}$  (100% and 83%, respectively) than of AUC (75% and 67%, respectively).<sup>38</sup> Others recently confirmed that there is a significant difference in  $K^{trans}$  values between patients with tumor progression and pseudoprogression, with higher values for the latter.<sup>39</sup> In addition, they were able to show a difference in mean  $V_e$  values, demonstrating a prognostic accuracy of 88% when a cutoff value of 0.873 was used.<sup>39</sup> However, the deficiency of uniform thresholds due to a lack of uniformity in data acquisition and pharmacokinetic models remains troublesome.

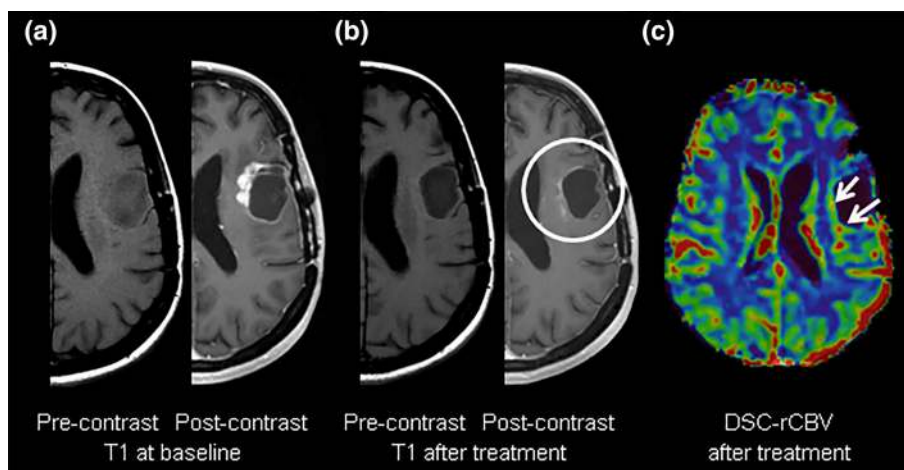


**FIGURE 5:** Pseudoresponse identified by dynamic susceptibility contrast (DSC). Patient with a recurrent glioblastoma with new contrast enhancement on T<sub>1</sub>-weighted MRI after completion of chemotherapy (a). The patient received second-line antiangiogenic treatment with bevacizumab. After the first course, follow-up MRI (b) showed a decrease in contrast-enhancing lesions (white circle), suggestive of apparent response. However, DSC demonstrated persisting high perfusion values (arrows) confirming the changes were due to pseudoresponse (c). Subsequent follow-up scans demonstrated an increase in contrast enhancement and rCBV and the patient deteriorated. DSC = dynamic susceptibility contrast, rCBV = relative cerebral blood volume.

ASL studies for treatment evaluation in GBM are limited. The previously mentioned meta-analysis identified only two ASL studies, reporting disappointing diagnostic accuracy.<sup>30,34,40</sup> Moreover, these studies showed large differences in sensitivity and specificity.<sup>30</sup> ASL demonstrates tumor progression as high rCBF values (Fig. 3). A higher imaging quality has been reported in ASL in comparison to DSC for the differentiation between tumor progression and pseudoprogression using rCBF values.<sup>41</sup> Although ASL and DSC were both capable of reliably differentiating between progression and pseudoprogression, DSC reached a higher diagnostic accuracy in this study.<sup>41</sup> However, another study suggested that ASL could outperform DSC when using a normalized CBF cutoff ratio of 1.3.<sup>31</sup>

## PSEUDORESPONSE

Due to unsatisfying survival rates, trials have investigated novel treatment strategies, including antiangiogenic agents. During antiangiogenic treatment a rapid decrease in contrast enhancement and peritumoral edema is often seen on conventional imaging.<sup>42</sup> These radiological changes are reported in 25–60% of the patients undergoing antiangiogenic treatment.<sup>43</sup> A first decrease in contrast enhancement and edema can be seen after several days. Mostly this radiological pattern goes together with a temporary improvement of clinical symptoms.<sup>44</sup> However, the decrease in contrast enhancement in pseudoresponse is not associated with a decrease in tumor or survival improvement.<sup>44</sup>

Antiangiogenic treatment can potentially focus on any of the proangiogenic factors involved in GBM neovascularization. However, most current strategies are aimed at vascular endothelial growth factor (VEGF) or its receptor. Most studied agents are bevacizumab, a recombinant monoclonal VEGF-A antibody, and cediranib, a pan-VEGF receptor tyrosine kinase inhibitor. Antiangiogenic treatment is thought to induce tumor hypoxia and temporarily normalize vascularization, thereby enhancing the delivery of chemotherapy and radiotherapy. Initial trial results were promising but included patients with pseudoresponse, hindering a reliable assessment of their value. Up to now, most randomized controlled trials studying antiangiogenic agents have failed to show a favorable effect on survival of GBM patients after exclusion of patients with pseudoresponse.<sup>45,46</sup> However, active phase III trials are still ongoing. Furthermore, pseudoresponse might also occur during treatment with immunotherapeutic agents, which are currently under investigation in many clinical trials.<sup>47</sup>

Pseudoresponse typically involves a rapid decrease in contrast enhancement on T<sub>1</sub> and FLAIR signal after administration of antiangiogenic agents. Perfusion MRI, however, can demonstrate persistent increased perfusion values within

the apparently responsive lesion (Fig. 5). One study aimed to distinguish true responders from nonresponders with DSC after treatment with a non-VEGF protein kinase inhibitor (enzastaurin) in addition to temozolomide.<sup>48</sup> The authors showed that responders demonstrated a decrease in DSC-derived peak height and an increase in percentage of signal recovery parameters.<sup>48</sup> The increase in percentage of signal recovery was suggestive of an improvement in vessel permeability due to enzastaurin. Contrary to these findings, a DSC study in 18 recurrent GBM patients did not find significant differences in absolute CBV values between true treatment responders and pseudoresponders.<sup>49</sup>

Rapid normalization of vessel permeability associated with antiangiogenic treatment has been demonstrated by early decreases in K<sup>trans</sup> using DCE perfusion.<sup>50,51</sup> This decrease in K<sup>trans</sup> was also associated with improvement of outcome in one study.<sup>51</sup> A phase II trial investigating the effect of adding cediranib to standard treatment showed an early decrease in K<sup>trans</sup> in all patients. Patients with an increased CBF showed a better outcome than stable or decreased perfusion following cediranib administration.<sup>52</sup>

To the best of our knowledge, no clinical ASL studies are currently available on differentiating responders of antiangiogenic treatment from pseudoresponders. However, in a preclinical study ASL-derived rCBF values decreased corresponding to a histological response after bevacizumab administration in a glioma rat model.<sup>53</sup>

## CURRENT CLINICAL PRACTICE

Perfusion MRI has proven to be useful in treatment evaluation in neuro-oncology. However, not all techniques are widely available. Two recent large international surveys were conducted among members of the American Society of Neuroradiology (ASNR) and European Society of Neuroradiology (ESNR).<sup>8,9</sup> Out of 195 institutions included in the ASNR survey, 151 offered perfusion MRI and 87% thereof included perfusion MRI in their standard neuro-oncology imaging protocol. Specifically for evaluating the presence of pseudoprogression and pseudoresponse, these percentages were 96% and 66%, respectively.<sup>8</sup> Results from the ESNR survey on glioma imaging practices in 220 institutions among 31 European countries showed that perfusion MRI is commonly utilized among European centers; perfusion MRI was implemented in the standard imaging protocol in 48% of the centers.<sup>9</sup> In both surveys, DSC was shown to be the most employed perfusion method (87% and 82% for the ASNR and ESNR, respectively) followed by DCE (41% and 29%) and ASL (35% and 12%).<sup>8,9</sup> However, only half of the centers that performed perfusion imaging performed quantitative analysis. In addition, the lack of postprocessing software was an important reason for not acquiring perfusion imaging.

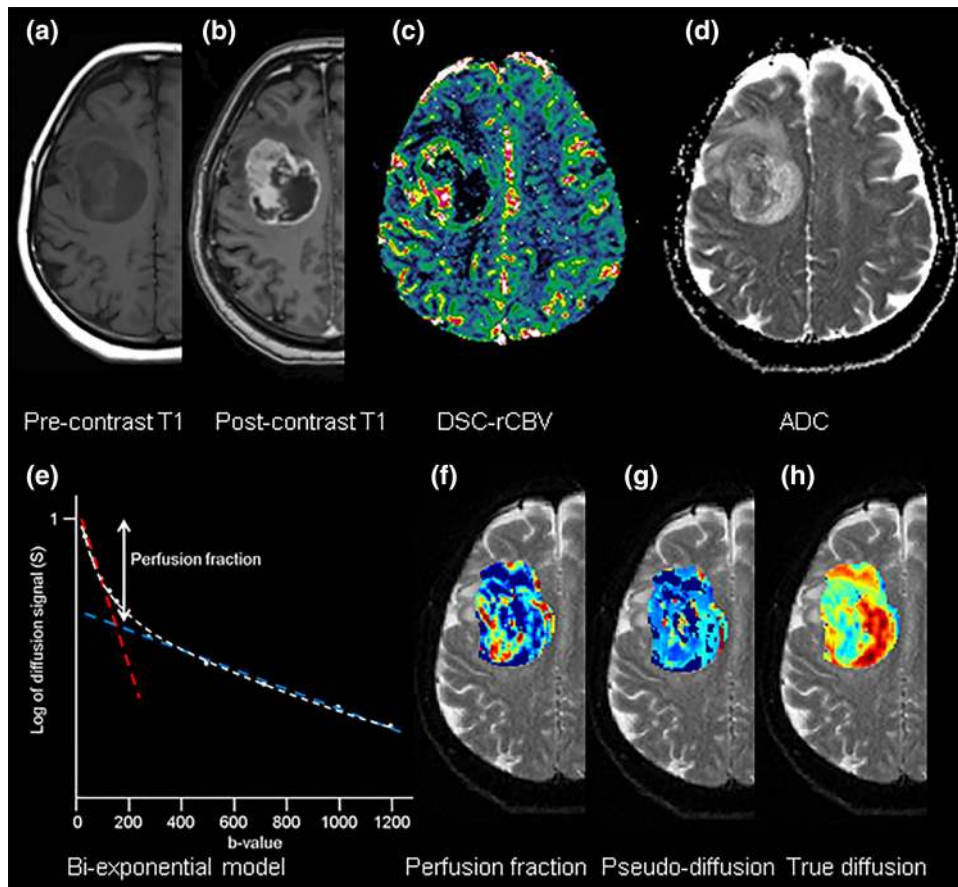


**FIGURE 6:** Intravoxel incoherent motion (IVIM) diffusion-weighted imaging in glioblastoma. MRI of a 64-year-old female with a right frontal glioblastoma as shown on pre- (a) and postcontrast  $T_1$ -weighted imaging (b). DSC demonstrated elevated perfusion at location of contrast enhancement (c) and diffusion-weighted imaging showed decreased ADC laterally due to increased cellularity and elevated ADC in the necrotic core (d). IVIM imaging uses a biexponential model of signal decay (e). The diffusion signal is demonstrated in white for different b-values. With IVIM this signal decay can be divided into the flow-related pseudodiffusion (red dotted line) and the true diffusion (blue dotted line). The perfusion fraction (f) results from the signal difference between pseudodiffusion and true diffusion. The perfusion fraction demonstrated similar results to DSC-rCBV (c). A pseudodiffusion map is also shown (g). IVIM-derived true diffusion maps (h) are comparable to ADC with elevated values in the necrotic core. ADC = apparent diffusion coefficient, DSC = dynamic susceptibility contrast, IVIM = intravoxel incoherent motion, rCBV = relative cerebral blood volume.

## NEW DEVELOPMENTS AND PERSPECTIVES

### Other Imaging Techniques

According to the consensus recommendations for a standardized brain tumor imaging protocol in clinical trials, the minimum required protocol includes conventional pre- and postcontrast 3D  $T_1$ -weighted, axial 2D  $T_2$ -weighted, and axial 2D  $T_2$ -weighted FLAIR sequences as well as axial 2D diffusion-weighted imaging.<sup>54</sup> Despite the higher diagnostic accuracy of diffusion-weighted imaging compared with conventional MRI for differentiating pseudoprogression from tumor progression, it is still inferior to perfusion MRI.<sup>30</sup> Considering the limitations of the standardized brain tumor imaging protocol the Response Assessment in Neuro-Oncology (RANO) working group recently recommended the use of amino positron emission tomography (PET) imaging in addition to MRI.<sup>55</sup> Amino PET is able to differentiate pseudoprogression from tumor progression with high sensitivity and specificity, but it is not known which amino tracer

has the best diagnostic accuracy and a meta-analysis is therefore wanted.<sup>55</sup> Furthermore, it has not been investigated if amino PET can outperform perfusion MRI in GBM treatment evaluation. However, hybrid PET/MR systems allow simultaneous assessment with amino PET and perfusion MRI and are therefore promising. Finally, perfusion computer tomography (CT) is capable of measuring rCBV and permeability surface-area product, comparable to  $K^{trans}$ .<sup>56,57</sup> CT could thus be used for glioblastoma treatment evaluation in case of MRI contraindications, despite its limited soft-tissue contrast and limited spatial resolution.

### New MRI Perfusion Techniques

Vessel architectural imaging (VAI) is a new perfusion technique based on the simultaneous acquisition of gradient-echo and spin-echo DSC images. Differences in susceptibility effects of the gradient-echo and spin-echo readouts cause a difference in the relaxation rate curves. Hemodynamic



properties such as oxygenation, vessel diameter, and flow rate influence the relaxation and induce a variability between the gradient-echo and spin-echo. In a study among 30 patients with recurrent GBM enrolled in a phase II trial with cediranib, normalization of microcirculation could be detected by VAI, showing its potential to identify treatment responders.<sup>58</sup> Moreover, illustrative case examples of VAI and its measurable parameters are included in the aforementioned study.<sup>58</sup>

Intravoxel incoherent motion (IVIM) is an advanced diffusion-weighted imaging technique. Many advanced diffusion-weighted imaging techniques exist,<sup>59</sup> but IVIM has the unique possibility of also allowing perfusion assessment (Fig. 6). It uses a biexponential model for diffusion calculation (Fig. 6d). Diffusion is influenced by microcirculatory perfusion, mainly affecting results among lower b values. Using a number of low b values the flow-related pseudodiffusion and perfusion fraction can be derived, which correspond well to DSC-derived CBV and CBF values.<sup>60</sup> So far, only one study has investigated the ability of IVIM to distinguish pseudoprogression from tumor progression in GBM patients using the 90<sup>th</sup> percentile values of IVIM-derived perfusion fraction.<sup>61</sup> The perfusion fraction was significantly higher in tumor progression compared with pseudoprogression. Currently, a study is under investigation to compare IVIM and ASL for the differentiation of tumor and pseudoprogression.<sup>62</sup>

### Analyses

Analysis of perfusion MRI can be done using many different methods, of which most are semiquantitative or are determined by arterial input function. A new postprocessing technique using wavelet-based reconstruction might further improve visual assessment, as background structures and vessels are better suppressed.<sup>63</sup> Furthermore, radiomics has the potential to improve complex analysis. Radiomics involves the mining of quantitative radiological features.<sup>64,65</sup> Radiomics has already demonstrated its prognostic value in differentiating pseudoprogression from tumor progression based on textural features of conventional MRI.<sup>66–68</sup> Studies including perfusion parameters in radiomics analyses for treatment evaluation in GBM are currently scarce, but preliminary data are promising.<sup>69</sup> Radiomic-derived features can also be combined with molecular and genetic data (radiogenomics).<sup>70</sup> Potentially, radiogenomics can be employed for the differentiation of pseudoprogression from tumor progression by differences in molecular signature.<sup>71</sup> A relationship between perfusion imaging-derived parameters and molecular tumor characteristics has been described earlier, with shown correlations between rCBV and epidermal growth factor receptor variant III (EGFRvIII) amplification.<sup>72</sup> However, more research is needed to establish clear genetic differences between pseudoprogression and tumor progression and their possible association with perfusion parameters. In addition, machine learning

allows automatic decision-making based on supervised or unsupervised computational learning in a training set. A study has shown that pseudoprogression can reliably be distinguished from tumor progression using a support vector machine learning method, with perfusion MRI parameters showing the highest sensitivity and specificity.<sup>73</sup>

## REMAINING QUESTIONS

### Standardization of Parameters

The generalizability and quantification of the different techniques are large hurdles to overcome for the incorporation of perfusion MRI in daily clinical care. Cutoff values for different perfusion parameters are not standardized and calculation thereof often requires manual input. Unfortunately, it is not possible to provide recommendations on optimal cutoff values considering the widespread thereof used throughout earlier studies (0.71–3.7) (see also our recent meta-analysis).<sup>30</sup> Future work should be aimed at validating cutoff values and standardized quantification of perfusion images allowing identification of the best cutoff for clinical implementation. Moreover, decisions about incorporating perfusion MRI in every follow-up protocol are to be made.<sup>4,54</sup> Currently, the imaging follow-up interval of treated GBM patients remains debatable and it is not known if adding perfusion MRI to every follow-up scan improves clinical decision-making. Finally, comparing perfusion parameters longitudinally in a patient is not straightforward, as the coregistration of subsequent follow-up scans remains challenging.<sup>74</sup>

### Role in New Treatments

In recent years, more and more interest has evolved toward the field of immunotherapy. Novel immune checkpoint blockers are currently under investigation in several phase III clinical trials. Promising agents include ipilimumab, a cytotoxic T lymphocyte-associated antigen 4 (CTLA-4) blocker, programmed cell death 1-receptor (PD1) blockers such as pembrolizumab or nivolumab, and genetically modified T-cells expressing chimeric antigen receptors (CAR-T therapy).<sup>75–77</sup> Although the long-term effects are not yet fully understood, treatment-induced inflammation and associated pseudoprogression have also been reported after immunotherapy. On conventional imaging both increases and decreases in contrast enhancement and edema have been observed among responders.<sup>47</sup> To aid in treatment evaluation for patients enrolled in clinical trials studying immunotherapeutic agents, the immunotherapy response assessment in neuro-oncology (iRANO) criteria have been established.<sup>47</sup> The iRANO thus far recommends the use of conventional MRI scans along with clinical criteria for evaluation of immunotherapy.<sup>47</sup> According to the iRANO criteria, the occurrence of a new lesion is not automatically classified as progressive disease. Clinically stable patients treated less than 6 months with the immunotherapeutic agent with the occurrence of a new lesion

require a second scan after 3 months.<sup>47</sup> It is unknown if perfusion imaging could overcome this potential delay, hence perfusion imaging is not yet incorporated in the iRANO recommendations. The added value of perfusion imaging GBM patients treated with immunotherapy should be further studied.

To reduce adverse events associated with conventional irradiation, proton beam therapy is becoming more available. Proton beam therapy allows more precise targeting of the tumor with maximum dose delivery to tumor and minimal damage to surrounding tissues compared with conventional photon therapy. Pseudoprogression can also be caused by proton therapy. A recent study among high-grade gliomas showed similar incidences of pseudoprogression between conventionally irradiated patients and patients receiving proton therapy.<sup>78</sup> However, little is known about pseudoprogression and the role of perfusion MRI for treatment follow-up in GBM patients treated with proton beam therapy.

## CONCLUSION

This review contributes to the growing body of evidence for the added value of perfusion MRI in the treatment evaluation of GBM. Perfusion MRI has the potential to overcome the shortcomings of conventional MRI and better distinguish tumor from treatment-induced processes such as pseudoprogression and pseudoresponse. DSC remains the best established perfusion method followed by DCE, both of which show comparable high diagnostic accuracy for differentiating tumor progression from pseudoprogression. The contrast-independent method ASL is promising, but studies on its role in GBM treatment evaluation are thus far limited. Quantification of perfusion images remains the largest hurdle to overcome for standardization of perfusion MRI in imaging protocols and future work should be aimed thereat.

## ACKNOWLEDGMENT

We thank dr. Hildebrand Dijkstra for providing the illustrative IVIM diffusion-weighted MRI case of Fig. 6.

## REFERENCES

- Stupp R, Mason WP, Van Den Bent MJ, et al. Radiotherapy plus concomitant and adjuvant temozolomide for glioblastoma. *N Engl J Med* 2005;352:10:987–996.
- Verma N, Cowperthwaite MC, Burnett MG, Markey MK. Differentiating tumor recurrence from treatment necrosis: A review of neuro-oncologic imaging strategies. *Neuro Oncol* 2013;15:515–534.
- Brandsma D, Stalpers L, Taal W, Sminia P, van den Bent MJ. Clinical features, mechanisms, and management of pseudoprogression in malignant gliomas. *Lancet Oncol* 2008;9:453–461.
- Thust SC, Bent MJ Van Den, Smits M. Pseudoprogression of brain tumors. *J Magn Reson Imaging* 2018;1–19.
- Ronca R, Benkheil M, Mitola S, Struyf S, Liekens S. Tumor angiogenesis revisited: Regulators and clinical implications. *Med Res Rev* 2017;37:1231–1274.
- Wang N, Jain RK, Batchelor TT. New directions in anti-angiogenic therapy for glioblastoma. *Neurotherapeutics* 2017;14:321–332.
- Carmeliet P, Jain RK. Angiogenesis in cancer and other diseases. *Nature* 2000;407:249–257.
- Dickerson E, Srinivasan A. Multicenter survey of current practice patterns in perfusion MRI in neuroradiology: Why, when, and how is it performed? *Am J Roentgenol* 2016;207:406–410.
- Thust SC, Heiland S, Falini A, et al. Glioma imaging in Europe? A survey of 220 centres and recommendations for best clinical practice. *Eur Radiol* 2018 [Epub ahead of print].
- Østergaard L. Principles of cerebral perfusion imaging by bolus tracking. *J Magn Reson Imaging* 2005;22:710–717.
- Essig M, Shiroishi MS, Nguyen TB, et al. Perfusion MRI: The five most frequently asked technical questions. *Am J Roentgenol* 2013;200:24–34.
- Welker K, Boxerman J, Kalnin A, Kaufmann T, Shiroishi M, Wintermark M. ASFN recommendations for clinical performance of MR dynamic susceptibility perfusion imaging of the brain. *AJNR Am J Neuroradiol* 2015;36:E41–E51.
- Suh CH, Kim HS. Multiparametric MRI as a potential surrogate endpoint for decision-making in early treatment response following concurrent chemoradiotherapy in patients with newly diagnosed glioblastoma? A systematic review and meta-analysis. *Eur Radiol* 2018;28:2628–2648.
- Leu K, Boxerman JL, Ellingson BM. Effects of MRI protocol parameters, preload injection dose, fractionation strategies, and leakage correction algorithms on the fidelity of dynamic-susceptibility contrast MRI estimates of relative cerebral blood volume in gliomas. *Am J Neuroradiol* 2017;38:478–484.
- Kluge A, Lukas M, Toth V, Pyka T, Zimmer C, Preibisch C. Analysis of three leakage-correction methods for DSC-based measurement of relative cerebral blood volume with respect to heterogeneity in human gliomas. *Magn Reson Imaging* 2016;34:410–421.
- Gahramanov S, Muldoon LL, Varallyay CG, et al. Pseudoprogression of glioblastoma after chemo- and radiation therapy: diagnosis by using dynamic susceptibility-weighted contrast-enhanced perfusion MR imaging with ferumoxytol versus gadoteridol and correlation with survival. *Radiology* 2013;266:842–852.
- Puig J, Blasco G, Essig M, et al. Albumin-binding MR blood pool contrast agent improves diagnostic performance in human brain tumour: Comparison of two contrast agents for glioblastoma. *Eur Radiol* 2013;23:1093–1101.
- Paldino MJ, Barboriak DP. Fundamentals of quantitative dynamic contrast-enhanced MR imaging. *Magn Reson Imaging Clin N Am* 2009;17:277–289.
- Sourbron SP, Buckley DL. Classic models for dynamic contrast-enhanced MRI. *NMR Biomed* 2013;26:1004–1027.
- Khalifa F, Soliman A, El-baz A, et al. Models and methods for analyzing DCE-MRI: A review. *Med Phys* 2014;41:124301.
- Keil VC, Mädler B, Gieseke J, et al. Effects of arterial input function selection on kinetic parameters in brain dynamic contrast-enhanced MRI. *Magn Reson Imaging* 2017;40:83–90.
- Grade M, Hernandez Tamames JA, Pizzini FB, Achten E, Golay X, Smits M. A neuroradiologist's guide to arterial spin labeling MRI in clinical practice. *Neuroradiology* 2015;57:1181–1202.
- Haller S, Zaharchuk G, Thomas DL, Lovblad K-O, Barkhof F, Golay X. Arterial spin labeling perfusion of the brain: emerging clinical applications. *Radiology* 2016;281:337–356.
- Alsop DC, Detre JA, Golay X, et al. Recommended implementation of arterial spin-labeled perfusion MRI for clinical applications: A consensus of the ISMRM Perfusion Study group and the European consortium for ASL in dementia. *Magn Reson Med* 2015;73:102–116.
- Amukotuwa SA, Yu C, Zaharchuk G. 3D pseudocontinuous arterial spin labeling in routine clinical practice: A review of clinically significant artifacts. *J Magn Reson Imaging* 2016;43:11–27.

26. Detre JA, Rao H, Wang DJJ, Chen YF, Wang Z. Applications of arterial spin labeled MRI in the brain. *J Magn Reson Imaging* 2012;35:1026–1037.
27. Abbasi AW, Westerlaan HE, Holtman GA, Aden KM, van Laar PJ, van der Hooft A. Incidence of tumour progression and pseudoprogression in high-grade gliomas: a systematic review and meta-analysis. *Clin Neuroradiol* 2017;1–11.
28. Lin AL, White M, Miller-Thomas MM, et al. Molecular and histologic characteristics of pseudoprogression in diffuse gliomas. *J Neurooncol* 2016;130:529–533.
29. Melguizo-Gavilanes I, Bruner JM, Guha-Thakurta N, Hess KR, Puduvali VK. Characterization of pseudoprogression in patients with glioblastoma: is histology the gold standard? *J Neurooncol* 2015;123:141–150.
30. van Dijken BRJ, van Laar PJ, Holtman GA, van der Hooft A. Diagnostic accuracy of magnetic resonance imaging techniques for treatment response evaluation in patients with high-grade glioma, a systematic review and meta-analysis. *Eur Radiol* 2017;4129–4144.
31. Ozsunar Y, Mullins ME, Kwong K, et al. Glioma recurrence versus radiation necrosis. A pilot comparison of arterial spin-labeled, dynamic susceptibility contrast enhanced MRI, and FDG-PET imaging. *Acad Radiol* 2010;17:282–290.
32. Wan B, Wang S, Tu M, Wu B, Han P, Xu H. The diagnostic performance of perfusion MRI for differentiating glioma recurrence from pseudoprogression. *Medicine* 2017;96:1–7.
33. Patel P, Baradaran H, Delgado D, et al. MR perfusion-weighted imaging in the evaluation of high-grade gliomas after treatment: A systematic review and meta-analysis. *Neuro Oncol* 2017;19:118–127.
34. Seeger A, Braun C, Skardelly M, et al. Comparison of three different MR perfusion techniques and MR spectroscopy for multiparametric assessment in distinguishing recurrent high-grade gliomas from stable disease. *Acad Radiol* 2013;20:1557–1565.
35. Barajas RF, Chang JS, Segal MR, Parsa AT, McDermott MW, Berger MS. Differentiation of recurrent glioblastoma multiforme from radiation necrosis after external beam radiation therapy with dynamic susceptibility-weighted contrast-enhanced perfusion MR imaging. *Radiology* 2009;253:486–496.
36. Barajas RF, Chang JS, Sneed PK, Segal MR, McDermott MW, Cha S. Distinguishing recurrent intra-axial metastatic tumor from radiation necrosis following gamma knife radiosurgery using dynamic susceptibility-weighted contrast-enhanced perfusion MR imaging. *Am J Neuroradiol* 2009;30:367–372.
37. Young RJ, Gupta A, Shah AD, et al. MRI perfusion in determining pseudoprogression in patients with glioblastoma. *Clin Imaging* 2013;37:41–49.
38. Bisdas S, Naegel T, Ritz R, et al. Distinguishing recurrent high-grade gliomas from radiation injury. A pilot study using dynamic contrast-enhanced MR imaging. *Acad Radiol* 2011;18:575–583.
39. Yoo R-E, Choi SH, Kim TM, et al. Dynamic contrast-enhanced MR imaging in predicting progression of enhancing lesions persisting after standard treatment in glioblastoma patients: a prospective study. *Eur Radiol* 2017;27:3156–3166.
40. Choi YJ, Kim HS, Jahng G-H, Kim SJ, Suh DC. Pseudoprogression in patients with glioblastoma: added value of arterial spin labeling to dynamic susceptibility contrast perfusion MR imaging. *Acta Radiol* 2013;54:448–454.
41. Xu Q, Liu Q, Ge H, et al. Tumor recurrence versus treatment effects in glioma. *Medicine* 2017;96:e9332.
42. Hygino da Cruz LC, Rodriguez I, Domingues RC, Gasparetto EL, Sorensen AG. Pseudoprogression and pseudoresponse: imaging challenges in the assessment of posttreatment glioma. *Am J Neuroradiol* 2011;32:1978–1985.
43. Wen PY, Macdonald DR, Reardon DA, et al. Updated response assessment criteria for high-grade gliomas: Response assessment in neuro-oncology working group. *J Clin Oncol* 2010;28:1963–1972.
44. Brandsma D, Van Den Bent MJ. Pseudoprogression and pseudoresponse in the treatment of gliomas. *Curr Opin Neurol* 2009;22:633–638.
45. Batchelor TT, Mulholland P, Neyns B, et al. Phase III randomized trial comparing the efficacy of cediranib as monotherapy, and in combination with lomustine, versus lomustine alone in patients with recurrent glioblastoma. *J Clin Oncol* 2013;31:3212–3218.
46. Wick W, Gorlia T, Bendszus M, et al. Lomustine and bevacizumab in progressive glioblastoma. *N Engl J Med* 2017;377:1954–1963.
47. Okada H, Weller M, Huang R, et al. Immunotherapy response assessment in neuro-oncology: A report of the RANO working group. *Lancet Oncol* 2015;16:e534–e542.
48. Essock-Burns E, Lupo JM, Cha S, et al. Assessment of perfusion MRI-derived patients with newly diagnosed glioblastoma. *Neuro Oncol* 2011;13:119–131.
49. Stadlbauer A, Pichler P, Karl M, et al. Quantification of serial changes in cerebral blood volume and metabolism in patients with recurrent glioblastoma undergoing antiangiogenic therapy. *Eur J Radiol* 2015;84:1128–1136.
50. Batchelor TT, Sorensen AG, di Tomaso E, et al. AZD2171, a pan-VEGF receptor tyrosine kinase inhibitor, normalizes tumor vasculature and alleviates edema in glioblastoma patients. *Cancer Cell* 2007;11:83–95.
51. Sorensen AG, Batchelor TT, Zhang WT, et al. A “vascular normalization index” as potential mechanistic biomarker to predict survival after a single dose of cediranib in recurrent glioblastoma patients. *Cancer Res* 2009;69:5296–5300.
52. Batchelor TT, Gerstner ER, Emblem KE, et al. Improved tumor oxygenation and survival in glioblastoma patients who show increased blood perfusion after cediranib and chemoradiation. *Proc Natl Acad Sci U S A* 2013;110:19059–19064.
53. Yun TJ, Cho HR, Choi SH, et al. Antiangiogenic effect of bevacizumab: Application of arterial spin-labeling perfusion MR imaging in a rat glioblastoma model. *Am J Neuroradiol* 2016;37:1650–1656.
54. Ellingson BM, Bendszus M, Boxerman J, et al. Consensus recommendations for a standardized brain tumor imaging protocol in clinical trials. *Neuro Oncol* 2015;17:1188–1198.
55. Albert NL, Weller M, Suchorska B, et al. Response assessment in Neuro-Oncology working group and European Association for Neuro-Oncology recommendations for the clinical use of PET imaging in gliomas. *Neuro Oncol* 2016;18:1199–1208.
56. Saito T, Sugiyama K, Ikawa F, et al. Permeability surface area product using perfusion computed tomography is a valuable prognostic factor in glioblastomas treated with radiotherapy plus concomitant and adjuvant temozolomide. *World Neurosurg* 2017;97:21–26.
57. Jia ZZ, Shi W, Shi JL, Shen DD, Gu HM, Zhou XJ. Comparison between perfusion computed tomography and dynamic contrast-enhanced magnetic resonance imaging in assessing glioblastoma microvasculature. *Eur J Radiol* 2017;87:120–124.
58. Emblem KE, Mouridsen K, Bjornerud A, et al. Vessel architectural imaging identifies cancer patient responders to anti-angiogenic therapy. *Nat Med* 2013;19:1178–1183.
59. Nilsson M, Englund E, Szczepankiewicz F, van Westen D, Sundgren PC. Imaging brain tumour microstructure. *Neuroimage* 2018;1–19.
60. Federau C, O'Brien K, Meuli R, Hagmann P, Maeder P. Measuring brain perfusion with intravoxel incoherent motion (IVIM): Initial clinical experience. *J Magn Reson Imaging* 2014;39:624–632.
61. Kim HS, Suh CH, Kim N, Choi C-G, Kim SJ. Histogram analysis of intravoxel incoherent motion for differentiating recurrent tumor from treatment effect in patients with glioblastoma: initial clinical experience. *AJNR Am J Neuroradiol* 2014;35:490–497.
62. Liu ZC, Yan LF, Hu YC, et al. Combination of IVIM-DWI and 3D-ASL for differentiating true progression from pseudoprogression of Glioblastoma multiforme after concurrent chemoradiotherapy: Study protocol of a prospective diagnostic trial. *BMC Med Imaging* 2017;17:10–16.

63. Huber T, Rotkopf L, Kunz W, et al. Wavelet-based reconstructions of dynamic susceptibility MR perfusion: a new method to visualize hyper-vascular brain tumours. *Insights Imaging* 2018;S209.
64. Gillies RJ, Kinahan PE, Hricak H. Radiomics: Images are more than pictures, they are data. *Radiology* 2016;278:563–577.
65. Pinker K, Shitano F, Sala E, et al. Background, current role, and potential applications of radiogenomics. *J Magn Reson Imaging* 2018;47:604–620.
66. Grossmann P, Narayan V, Chang K, et al. Quantitative imaging biomarkers for risk stratification of patients with recurrent glioblastoma treated with bevacizumab. *Neuro Oncol* 2017;19:1688–1697.
67. Tiwari P, Prasanna P, Wolansky L, et al. Computer-extracted texture features to distinguish cerebral radio necrosis from recurrent brain tumors on multi-parametric MRI—A feasibility study. *AJNR Am J Neuroradiol* 2016;37:2231–2236.
68. Booth TC, Larkin TJ, Yuan Y, et al. Analysis of heterogeneity in T2-weighted MR images can differentiate pseudoprogression from progression in glioblastoma. *PLoS One* 2017;12:1–20.
69. Elshafeey N, Kotrotsou A, Giniembra Camejo D, et al. Multicenter study to demonstrate radiomic texture features derived from MR perfusion images of pseudoprogression compared to true progression in glioblastoma patients. *J Clin Oncol* 2017;35(Suppl):2016–2016.
70. Ellingson BM. Radiogenomics and imaging phenotypes in glioblastoma: novel observations and correlation with molecular characteristics. *Curr Neurol Neurosci Rep* 2015;15.
71. Qian X, Tan H, Zhang J, et al. Identification of biomarkers for pseudo and true progression of GBM based on radiogenomics study. *Oncotarget* 2016;7.
72. Tykocinski ES, Grant RA, Kapoor GS, et al. Use of magnetic perfusion-weighted imaging to determine epidermal growth factor receptor variant III expression in glioblastoma. *Neuro Oncol* 2012;14:613–623.
73. Hu X, Wong KK, Young GS, Guo L, Wong ST. Support vector machine multiparametric MRI identification of pseudoprogression from tumor recurrence in patients with resected glioblastoma. *J Magn Reson Imaging* 2011;33:296–305.
74. van der Hooft A, Yan JL, Larkin TJ, Boonzaier NR, Matys T, Price SJ. Validation of a semi-automatic co-registration of MRI scans in patients with brain tumors during treatment follow-up. *NMR Biomed* 2016;29:882–889.
75. Galldiks N, Kocher M, Langen KJ. Pseudoprogression after glioma therapy: an update. *Expert Rev Neurother* 2017;17:1109–1115.
76. Reardon DA, Freeman G, Wu C, et al. Immunotherapy advances for glioblastoma. *Neuro Oncol* 2014;16:1441–1458.
77. Bagley SJ, Desai AS, Linette GP, June CH, O'Rourke DM. CAR T-cell therapy for glioblastoma: recent clinical advances and future challenges. *Neuro Oncol* 2018;1–10.
78. Bronk JK, Guha-Thakurta N, Allen PK, Mahajan A, Grosshans DR, McGovern SL. Analysis of pseudoprogression after proton or photon therapy of 99 patients with low grade and anaplastic glioma. *Clin Transl Radiat Oncol* 2018;9:30–34.